

## Climate-Driven Variability and Trends in Mountain Snowpack in Western North America\*

PHILIP W. MOTE

*Climate Impacts Group, Center for Science in the Earth System, University of Washington, Seattle, Washington*

(Manuscript received 21 November 2005, in final form 17 February 2006)

### ABSTRACT

Records of 1 April snow water equivalent (SWE) are examined here using multiple linear regression against reference time series of temperature and precipitation. This method permits 1) an examination of the separate roles of temperature and precipitation in determining the trends in SWE; 2) an estimation of the sensitivity of SWE to warming trends, and its distribution across western North America and as a function of elevation; and 3) inferences about responses of SWE to future warming. These results emphasize the sensitivity to warming of the mountains of northern California and the Cascades of Oregon and Washington. In addition, the contribution of modes of Pacific climate variability is examined and found to be responsible for about 10%–60% of the trends in SWE, depending on the period of record and climate index.

### 1. Introduction

In most river basins of the West, especially in Washington, Oregon, and California, snow (rather than man-made reservoirs) is the largest component of water storage; hence, the West is (to varying degrees) vulnerable to climatic variations and changes that influence spring snowpack.

Since the midtwentieth century, as numerous studies have documented, important changes have occurred in hydrological properties in the West. In most of the West, these changes include trends toward earlier snowmelt-driven streamflow (Cayan et al. 2001; Stewart et al. 2005) that are more pronounced at lower elevation (Regonda et al. 2005), reduced flow in June and increased flow in March (Stewart et al. 2005), reduced spring snow water equivalent (SWE) (Mote 2003a; Mote et al. 2005), and reduced frequency of low-elevation snowfall (Groisman et al. 2004; Scott and Kaiser 2004; Knowles et al. 2006). Simulating the West's hydrology on a daily time scale from 1915 to 2003,

Hamlet et al. (2005) showed that most of the large-scale declines in snowpack and shifts in snowmelt runoff are related to temperature trends.

The present paper uses climate data from nearby stations to evaluate the sensitivity to temperature and precipitation of 1 April SWE at nearly 1000 locations in the West. Multiple linear regression is used to reconstruct SWE using only the climate variables, permitting a separation of the influences of temperature and precipitation on the observed trends. The role of Pacific climate patterns in the observed trends in SWE is also examined.

### 2. Data

As in Mote et al. (2005), snow course data through 2002 were obtained from the Water and Climate Center of the U.S. Department of Agriculture's Natural Resources Conservation Service (NRCS; [www.wcc.nrcs.usda.gov/snow/snowhist.html](http://www.wcc.nrcs.usda.gov/snow/snowhist.html)) for most states in the United States, from the California Department of Water Resources for California (<http://cdec.water.ca.gov>), and from the Ministry of Water, Land, Air, and Parks for British Columbia (<http://www.env.gov.bc.ca/rfc/>). In some instances, manual snow courses have been replaced by automated snow telemetry (SNOTEL) instruments; where overlap was sufficient to estimate the relationship between the snow course and SNOTEL estimates, NRCS provides two time series with back-

---

\* Joint Institute for the Study of Atmosphere and Ocean Contribution Number 1134.

---

*Corresponding author address:* Philip W. Mote, Climate Impacts Group, Center for Science in the Earth System, University of Washington, Box 354235, Seattle, WA 98195.  
E-mail: [philip@atmos.washington.edu](mailto:philip@atmos.washington.edu)



FIG. 1. Map of study area including major features and locations of certain snow courses mentioned in the text.

and forward-estimated values,<sup>1</sup> and we use both. In total 995 snow records span the time period 1960–2002 and are used here. Results for other periods of record (e.g., 1935–2002) are also shown, and results for 1 March and 1 May are examined but not shown.

For each snow course location, reference time series of temperature and precipitation are composed by combining observations at the five nearest climate stations for the months November through March, which roughly correspond to the snow accumulation season. These climate observations are drawn from the U.S. Historical Climate Network (USHCN; Karl et al. 1990) and from the Historical Canadian Climate Database (HCCD; Vincent and Gullett 1999), and the process of selecting and combining station records into reference time series is as described by Mote (2003a). The terrain and other geographic details are shown in Fig. 1.

### 3. Regression analysis

The 1 April SWE represents a cumulative, simplified summary of the previous several months' weather: de-

<sup>1</sup> That is, estimated values for the discontinued snow course have been derived for the years since it ended, and estimated values for the SNOTEL measurements have been derived for the period before it began. In most cases the mean values are different, but trends are similar. This affects about 10% of the data points.

position of snow, melting or ablation of snow, and rain events that may either partially melt the snow or be absorbed in the snowpack, increasing SWE. This simplified summary of weather will be represented in different fashions by 1 April SWE and by the mean temperature  $T$  and precipitation  $P$  during the snow accumulation season, taken here as the months November through March. We explore here how successfully the seasonal means of  $T$  and  $P$  at the nearest set of five climate stations can represent the observed interannual variability  $SWE(t)$  of mountain SWE for each year  $t$ , using the regression equation

$$SWE(t) = a_p P(t) + a_T T(t) + \varepsilon(t), \quad (1)$$

where  $a_p$  and  $a_T$  are the regression coefficients for precipitation  $P(t)$  and temperature  $T(t)$ , respectively, and  $\varepsilon$  is the residual at year  $t$  (see, e.g., von Storch and Zwiers 1999, p. 160ff, for a description of regression analysis.) After determining the regression coefficients, we derive  $S(t) \equiv \max[a_p P(t) + a_T T(t), 0]$ . In words,  $S(t)$  represents the variability associated (via regression) with the precipitation and temperature at the nearest climate stations but is not permitted to be negative. Three examples are given in Fig. 2. Emerald Lake has the highest correlation (0.95) between  $SWE(t)$  and  $S(t)$  of any snow course in the West: its 1 April SWE is determined almost entirely by total seasonal precipitation, and it is uncorrelated with temperature owing to its exceptionally high elevation. The simulated trend over the period of record (+7 cm or +8%) is fairly close to the observed trend (−3 cm or −3%) and both are statistically indistinguishable from zero.

Fish Lake, Oregon, has one of the highest correlations with temperature (−0.66) and has correspondingly shown a very large decline. On several occasions the observed SWE there was zero, as happens at many locations in the Cascades; but only twice (1934 and 1977, both exceptionally warm dry winters) does  $S(t)$  reach zero. Because the simulated variance is always less than the observed variance,  $S(t)$  tends to be too high at low values and too low at high values (see Fig. 2, right) and the simulated trends are usually smaller than the observed trends, as illustrated at Fish Lake.

At some sites, this regression approach does poorly at characterizing the interannual variations. For the West as a whole, a total of 61 (6%) snow course/SNOTEL locations have a correlation<sup>2</sup> between  $SWE(t)$  and  $S(t)$  that is less than 0.4 (Fig. 3). Big South, Colorado, is an example of such a location—only a handful of sites

<sup>2</sup> For  $n = 41$  the critical value of the correlation coefficient is 0.254 at  $\alpha = 0.05$ .

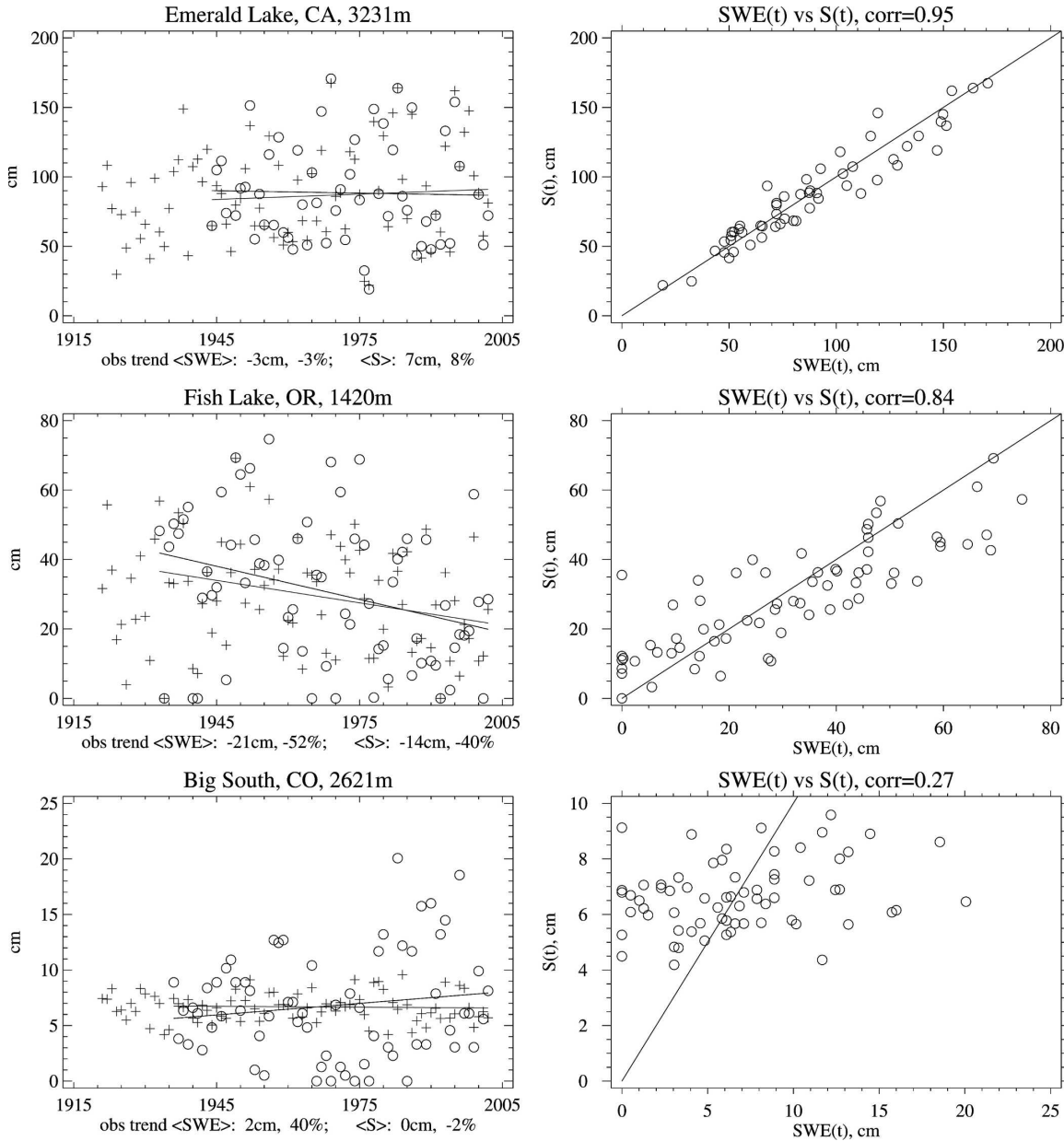


FIG. 2. (left) 1 Apr SWE as observed (circles) and as represented using regression on Nov–Mar temperature and precipitation at nearby USHCN (climate) stations (+), for three locations. Each time series also includes a linear fit over the period of record of the snow data. (right) Scatterplots of the observed SWE and  $S(t)$  [see Eq. (1)], along with the 1:1 line. Emerald Lake is insensitive to temperature and has shown very little decline; Fish Lake has a correlation with temperature of  $-0.66$  and shows a large decline related to the warming, in common with other temperature-sensitive areas. Big South has one of the lowest correlations with  $S(t)$ .

have correlations as low as 0.3. The variance explained is quite small, so the trends in climate-derived SWE are necessarily small and unrepresentative of observed trends in such cases, in this case of a substantial positive (40.4%) trend owing to increases in precipitation there (note also the low mean SWE at Big South.)

To visualize the correlations between SWE and the reference time series of temperature and precipitation

at each location, Fig. 3 plots the correlations as a scatterplot. The mean correlation with precipitation is 0.65, and half the values fall between 0.53 and 0.81. The mean correlation with temperature is  $-0.22$ , and half the values fall between  $-0.10$  and  $-0.36$ . Many of the locations exhibiting very high correlations with precipitation (like Emerald Lake; Fig. 2) are found in the highest, coldest locations in the Sierra Nevada and the

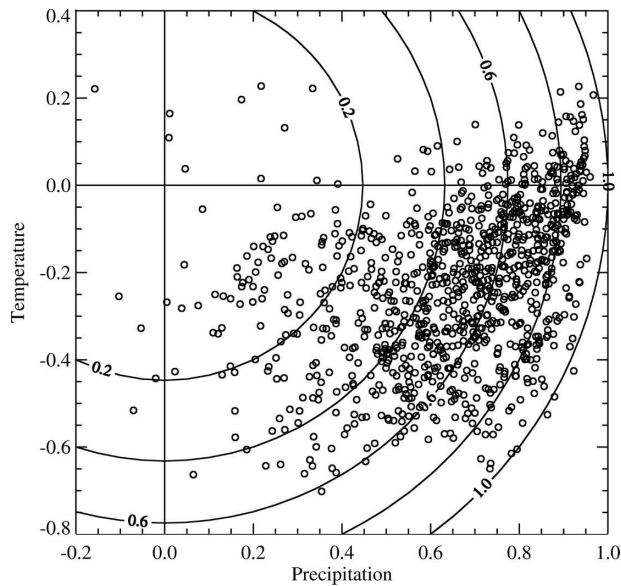


FIG. 3. Each small circle marks the correlations between 1 Apr SWE at one of the 995 snow course locations and the reference time series of Nov–Mar precipitation ( $x$  axis) and temperature ( $y$  axis). Contours indicate the quantity  $(r_T^2 + r_P^2)$ , an approximation of the variance explained.

Rockies. The ones with large (negative) correlation with temperature are generally found in the Cascades and the mountains of northern California and also in the Southwest (see Fig. 4 of Mote et al. 2005). A handful of sites have negative correlations with precipitation; two are in northeastern Oregon and three are in southern British Columbia. The reference time series of precipitation at these sites may not be a good representation of actual precipitation owing to topography and distance. A larger number of sites have positive correlation with temperature, which is more physically plausible, especially when we examine where these sites are found.

Temperature sensitivity—or correlation with temperature—is clearly dependent on elevation, especially for California (Fig. 4). The average correlation is near zero above about 2500 m and grows increasingly negative at lower elevations, exceeding  $-0.5$  below about 1800 m. As we will see shortly, most of the low-elevation and most temperature-sensitive snow courses in California lie in the northern half of the state.

Using the regression coefficients  $a_p$  and  $a_T$ , we can explore the roles of temperature and precipitation trends in producing observed trends in SWE. That is, evaluating the long-term trends of each term in Eq. (1) permits a comparison of the separate components  $a_p \langle P \rangle$  and  $a_T \langle T \rangle$ , where  $\langle Y \rangle$  indicates the linear trend in  $Y(t)$ . Maps of  $\langle SWE \rangle$ ,  $a_p \langle P \rangle$ ,  $a_T \langle T \rangle$ , and

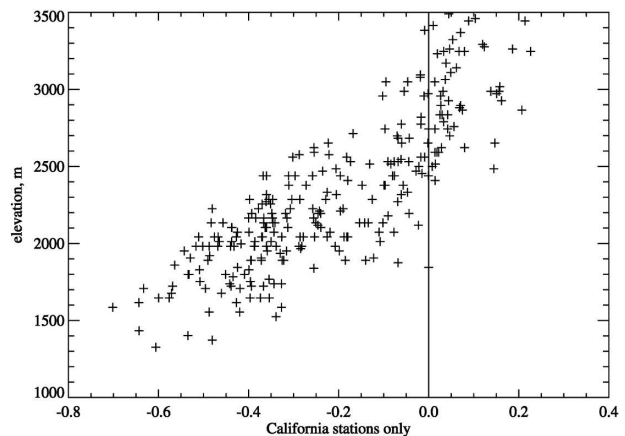


FIG. 4. Correlation between 1 Apr SWE and Nov–Mar temperature at each snow course location in California, plotted as a function of snow course elevation.

$\langle S \rangle = a_p \langle P \rangle + a_T \langle T \rangle$  are shown in Fig. 5 for the period 1960–2002. As noted previously for the periods of record 1950–97 (Mote et al. 2005) and 1916–2003 (Hamlet et al. 2005), observed trends in 1 April SWE over the period of record 1960–2002 are also predominantly negative: in fact, the fraction of sites having negative trends (76%) is approximately the same regardless of period of record and is roughly the same for the gridded output of the Variable Infiltration Capacity (VIC) hydrologic model and for the unevenly distributed snow course sites.

Comparing observed trends (Fig. 5a) with trends in  $\langle S \rangle$  (Fig. 5b) provides an indication of the degree to which climate variability can explain the observed trends in SWE. Broadly, the sign and spatial distribution of trends agree, with correlations between  $\langle SWE \rangle$  and  $\langle S \rangle$  of 0.71. As observed, the largest absolute trends are found in the Cascades of Oregon and the mountains of northern California, as well as parts of the Rockies; positive trends prevail in the southern Sierra Nevada mountains.

The largest trends occurred in the Cascades and the mountains of northern California and were evidently a result of both temperature and precipitation trends over this interval. Modeling work (Hamlet et al. 2005) suggests that temperature slightly predominates over this interval but that the declines over the longer 1916–2003 interval were almost entirely due to temperature trends.

The quantity  $a_T \langle T \rangle$  (Fig. 5c) is almost everywhere negative, reflecting the predominance of negative values of  $a_T$  (except at a few very high-elevation locations; see Fig. 4) and positive values of  $\langle T \rangle$ , and values of  $a_T \langle T \rangle$  are particularly large in the Cascades and the mountains of northern California. The field  $a_p \langle P \rangle$



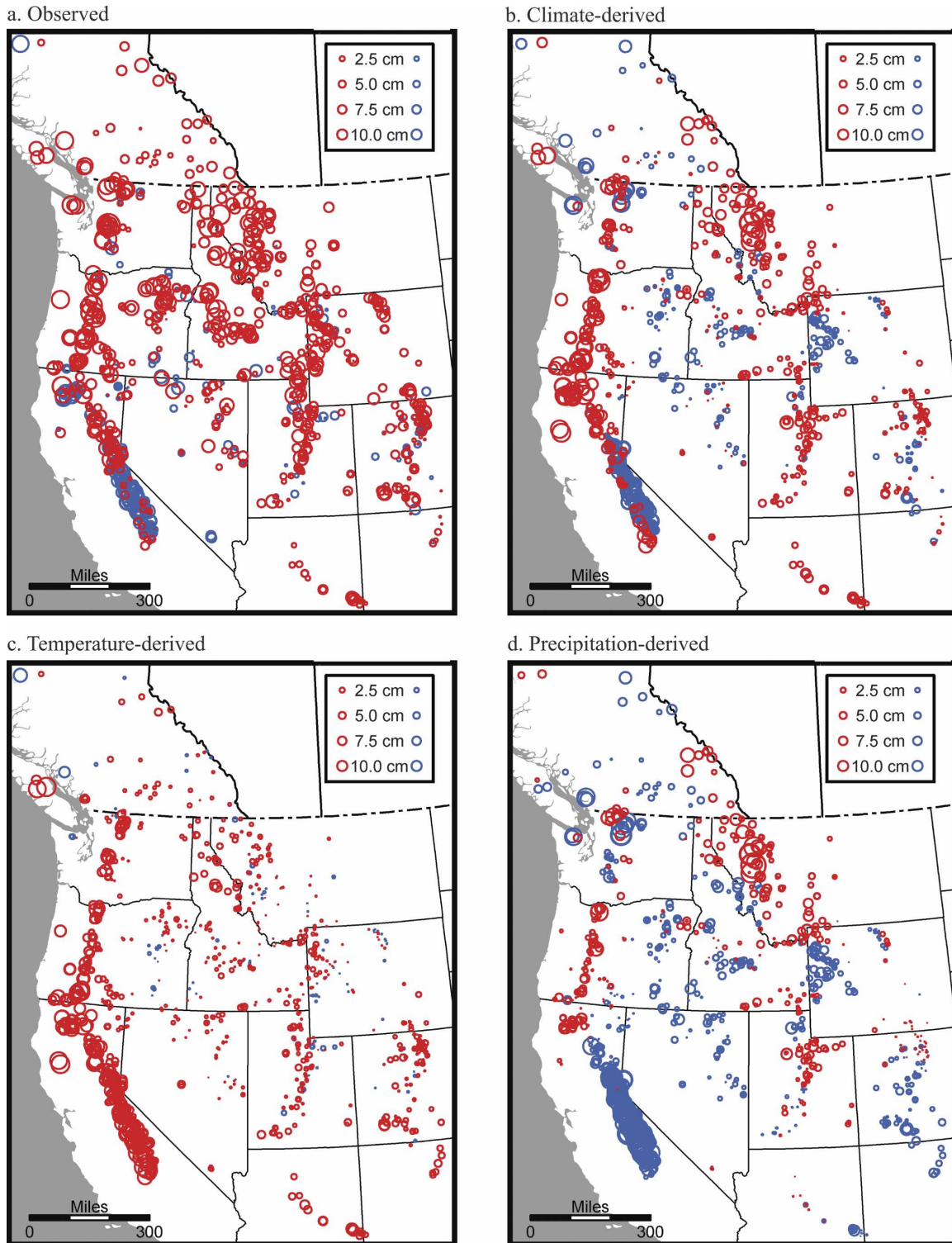


FIG. 5. Trends in 1 Apr SWE over the 1960–2002 period of record: (a) directly from snow course observations; (b)  $\langle S \rangle = a_p \langle P \rangle + a_T \langle T \rangle$ ; (c)  $a_T \langle T \rangle$ ; and (d)  $a_p \langle P \rangle$ . Positive trends are shown in blue and negative in red, by the scale indicated in the legend.

(Fig. 5d) is much more heterogeneous, with roughly equal numbers of positive and negative values; the typical scale of a patch of the same sign is on the order of 500 km.

Discrepancies in sign exhibited in Fig. 5b have a positive bias and tend to be clustered. Overall, the fraction of positive trends in  $S$  is much higher (42%) than for observations (24%). Discrepancies in sign occur predominantly in western Wyoming, eastern Oregon, southwestern Idaho, and Nevada, but there are none in Arizona and almost none in Washington, New Mexico, western Oregon, or Montana.

There are several possible causes of differences in sign between  $\langle SWE \rangle$  and  $\langle S \rangle$ :

- 1) changes in land cover at a snow course (e.g., growth of forest canopy) that would introduce a nonclimate trend in  $\langle SWE \rangle$ ;
- 2) trends in precipitation or temperature at the snow course location that do not match those at the lower-elevation stations used to form the reference time series;
- 3) changes in site characteristics at the reference climate stations such that the trends  $\langle T \rangle$  and  $\langle P \rangle$  are not representative of the true climate trends; and
- 4) other factors, like sensitivity to wind direction, that may have a time-dependent influence on the regression coefficients  $a_T$  and  $a_P$ .

Anecdotal evidence from snow surveyors suggests that possible cause 1 is a factor at some locations, though not generally the dominant factor. No systematic documentation of changes in site characteristics has been compiled. Tests with the VIC hydrology model and paired-catchment comparisons suggest that even drastic changes in land cover (clearcut logging) have an effect on hydrology that is secondary to that of climate (Bowling et al. 2000).

The second factor has been the subject of much recent research, at least for temperature (e.g., Diaz and Bradley 1997; Pepin and Seidel 2005), but most find little evidence that trends in temperature in high-elevation areas are significantly different from those in low elevations. Algorithms that relate temperature and precipitation to elevation for producing gridded climate data (Daly et al. 1994; Hamlet and Lettenmaier 2005) assume constant lapse rates in most conditions, ensuring that trends in temperature and precipitation at high elevation will be locked to those at low elevation, and hence are not suitable for evaluating this question. In mountainous areas, surface trends have been larger than free-air trends except at sites well exposed to the free atmosphere [which Pepin and Seidel (2005) called

mountaintop sites]. Knowles et al. (2006) found a slight increase of temperature trend with elevation for the western United States, but these were in cooperative weather data, which were uncorrected for station moves, etc., as in the USHCN. Far more difficult than determining how temperature trends depend on elevation is determining how precipitation trends may depend on elevation: obviously the absolute trends will usually be larger at higher, wetter locations, but a variety of local and synoptic-scale factors could produce different relative trends at different altitudes, and in fact even at similar elevations the trends in precipitation at nearby locations can be quite different (Mote 2003b). Hence we cannot evaluate to what extent the discrepancies between  $\langle SWE \rangle$  and  $\langle S \rangle$  may result from different climate trends at lower and higher elevations.

The third factor should be minimal, as the USHCN and HCCD datasets have been compiled and adjusted with precisely these factors in mind. In addition, the averaging of five climate stations to form a reference time series should further reduce the role of any uncorrected site changes.

Despite the concerns about these and other discrepancies, this simple regression approach clearly has some merits in diagnosing the changes in SWE that have been observed. In particular, it corroborates the findings of Hamlet et al. (2005) that temperature and precipitation both played a role in the recent decline of snowpack in the Cascades.

#### 4. Latitude–altitude transect

The largest absolute trends, largest relative trends, and greatest sensitivity to temperature generally are found on the coastal cordillera, the string of mountains from coastal British Columbia through the Cascades and Olympics, the coastal mountains of Oregon and northern California, and the northern Sierra Nevada. In the southern Sierra Nevada mountains, mean elevations are so much higher that despite their low latitude they are cold enough to accumulate substantial snowpack. To visualize the behavior of SWE in these critically important mountains, Fig. 6 shows a transect of snow course locations in California and in Washington, Oregon, and British Columbia west of 120° longitude (the meridian of the California–Nevada border north of Lake Tahoe).

Several observations emerge when looking at the snow course data from this perspective. First, the elevation of snow courses declines with latitude; it turns out that the slope of the distribution of snow courses roughly follows an isotherm, approximately 1 km in altitude per 7.3° latitude. [The isotherms were deter-

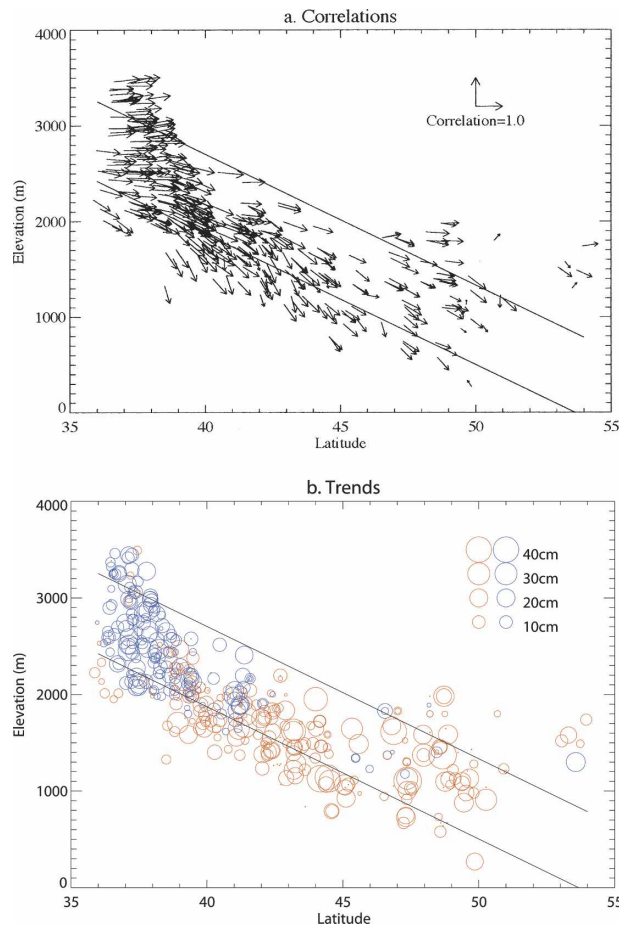


FIG. 6. Transect along the western cordillera of (a) correlations between 1 Apr SWE and Nov–Mar precipitation ( $x$  direction) and temperature ( $y$  direction), with unit correlations shown in the legend. Sloping lines are the  $0^{\circ}$  and  $-5^{\circ}\text{C}$  isotherms. (b) Linear trends in 1 Apr SWE over the 1960–2002 period of record.

mined by multiple linear regression on latitude and altitude, using December through February mean temperatures at the snow course locations from the Precipitation-Elevation Regression on Independent Slopes Model (PRISM) dataset (Daly et al. 1994; see Mote et al. 2005).] The exception to this distribution is in the southern Sierra Nevada, where a large area of the mountain range and a large number of snow courses are higher than 3000 m, well above the  $-5^{\circ}\text{C}$  isotherm that defines the highest elevation of snow courses farther north.

The correlations with precipitation and temperature are clearly dependent on elevation (Fig. 6a). At most latitudes, low-elevation locations (those at or below the  $0^{\circ}\text{C}$  isotherm) have high negative correlation with temperature and lower correlation with precipitation; traveling higher in elevation reduces the magnitude of the correlation with temperature and increases the correla-

tion with precipitation. At Antelope Springs, California (latitude  $38.5^{\circ}\text{N}$ , elevation 1326 m) 1 April SWE is determined almost entirely by temperature. In the southern Sierra Nevada mountains, as one travels up past the  $-5^{\circ}\text{C}$  isotherm the correlations with temperature go from negative to weakly positive, indicating that at these rare, very cold locations the warmest winters merely increase the moisture content of the air without increasing the risk that precipitation falls as rain (see also Fig. 4). Some of the locations in British Columbia (latitude  $>49^{\circ}\text{N}$ ) have very small correlation, which may reflect the sparsity of climate stations there.

Trends in 1 April SWE are also easier to interpret in this latitude–altitude transect (Fig. 6b). North of  $40^{\circ}\text{N}$ , negative trends prevail and positive trends tend to be found only at higher elevation. South of  $40^{\circ}\text{N}$ , positive trends prevail, but there are also negative trends mostly at lower elevation. Some of the largest absolute losses in SWE are found at lower elevations, even though mean SWE there is typically less than at higher elevations. That is, relative losses have been quite large—in excess of 80%—at low elevations, especially in Oregon (see Figs. 1 and 2 of Mote et al. 2005).

## 5. Connections to climate variability over the Pacific Ocean

Patterns of variability over the Pacific Ocean have known influences on winter and spring climate of the West. Statistical connections between snowpack and any index of climate variability  $X(t)$  can be established based on interannual fluctuations and used to deduce the role of  $X$  in longer-term trends, using the relationship

$$\text{SWE}(t) = a_X X(t) + \varepsilon(t) \quad (2)$$

[where, as in Eq. (1),  $a_X$  is the regression coefficient of SWE at each snow course location,  $X(t)$  is an annually varying index, and  $\varepsilon(t)$  is a residual time series] from which

$$\langle \text{SWE} \rangle_X = a_X \langle X \rangle, \quad (3)$$

that is, the portion of trend in SWE attributable to  $X$  is simply the product of the trend in  $X$  and the local regression coefficient. Note that this does not presume that the trend in residuals is zero, and note also that if  $\langle X \rangle$ , the trend in  $X$ , is zero over a particular interval, then by definition  $\langle \text{SWE} \rangle_X = 0$ . This is not the case for the trends examined here. In this portion of the study, each set of statistics was calculated for starting years at 5-yr intervals from 1935 to 1965 and for months March, April, and May, to examine the effects of period of record and of seasonality on the results.

For climate indices, several candidates are available that could influence SWE on decadal time scales. Pa-

cific decadal oscillation (PDO; e.g., Mantua et al. 1997) and El Niño–Southern Oscillation (ENSO) are both indices of variability in sea surface temperature in different regions. ENSO has well-documented influences on 1 April SWE in much of the West, with warm phase associated with lower snowpack in the Northwest and higher snowpack in the Southwest (Clark et al. 2001; their analysis of ENSO influence will not be repeated here).

Accounting for these patterns is important in understanding trends in SWE, especially since the period of most abundant snow course observations since 1945 corresponds approximately with a shift from predominantly cool phase PDO (relatively high snowpack and streamflow in the Northwest, opposite in the Southwest) during 1945–76 to predominantly warm phase PDO (low snowpack and streamflow) from 1977 to perhaps 1998.

Another measure of Pacific climate variability, one based not on properties of the ocean but of the atmosphere, is the North Pacific Index (NPI; Trenberth and Hurrell 1994), defined as the mean atmospheric sea level pressure over the region 30°–60°N, 160°E–140°W. PDO and NPI are weakly correlated ( $r = 0.30$ ) during the 1900–2002 period of record and share similar spectral characteristics with statistically significant ( $\alpha = 0.05$ ) interdecadal variability; PDO has higher lag-1 autocorrelation (0.40 versus 0.22). Both PDO and NPI have nonzero trends over the period of record of the snow courses, roughly since 1930 (Fig. 7); while the magnitude of the trends depends on the starting year, the sign is consistent for all starting years. Both indices reflect the late-twentieth-century trend toward a deeper Aleutian low. Though the PDO had predominantly positive values in 1925–45 and 1977–95, and predominantly negative values in 1945–76, since 1995 the index has changed sign frequently; in fact, the pattern of North Pacific variability has changed from predominantly first empirical orthogonal function (EOF1) (PDO) to predominantly EOF2 in the early 1990s (Bond et al. 2003).

The two indices, PDO and NPI, influence SWE over different spatial domains (Fig. 8). The general pattern of correlations is for SWE in the Northwest to be positively correlated with NPI and negatively correlated with PDO, and the opposite in the Southwest, but the dividing line between positive and negative correlations is quite different for the two indices. For PDO, it runs diagonally from northern California through central Idaho to the Montana–Wyoming border. For NPI, it runs more east–west from central California. Interesting details about these differences will emerge when we examine the correlations again as a latitude–altitude

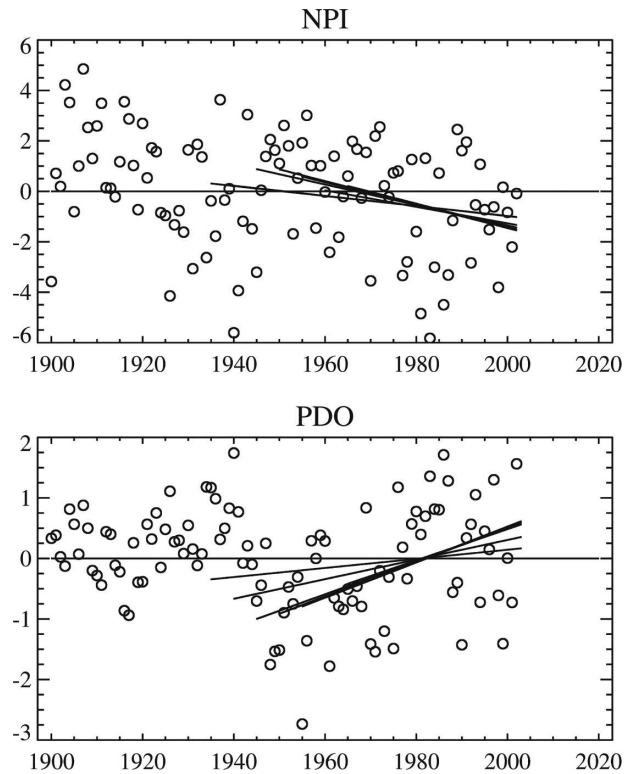


FIG. 7. Winter (Oct–Mar) average values of (top) the North Pacific Index and (bottom) the Pacific Decadal Oscillation index, along with linear fits for data spanning 1935–2002, 1940–2002, . . . 1965–2002.

transect. Correlations between SWE and NPI are generally larger than between SWE and PDO, and far more are positive. The starting year has very little influence on the correlation; for instance, the mean absolute difference between correlations of PDO and 1 April SWE for 1935–2002 and 1965–2002 (for stations with data 1935–2002) is only 0.07.

The quantities  $\langle \text{SWE} \rangle_{\text{PDO}}$  and  $\langle \text{SWE} \rangle_{\text{NPI}}$  for 1960–2002 are plotted in Figs. 8c,d, using the same scale as Fig. 5. These large-scale climate patterns clearly help explain some portion of the negative trends in the northern snow courses and also some portion of the positive trends in the southern snow courses. NPI is particularly helpful at explaining the downward trends in the northwestern snow courses, and PDO is helpful at explaining the upward trends in the central and southern Sierras.

From the maps it is difficult to evaluate the fraction of trend explained by PDO or NPI, so in Fig. 9 we show a scatterplot of the observed trend (Fig. 5a) against the quantity shown in Fig. 8d,  $\langle \text{SWE} \rangle_{\text{NPI}}$ , along with the  $y = x$  line and two least squares linear fits passing through the origin, one for snow courses in the Northwest (latitude  $>42^\circ$ , longitude  $>120^\circ$ , points repre-



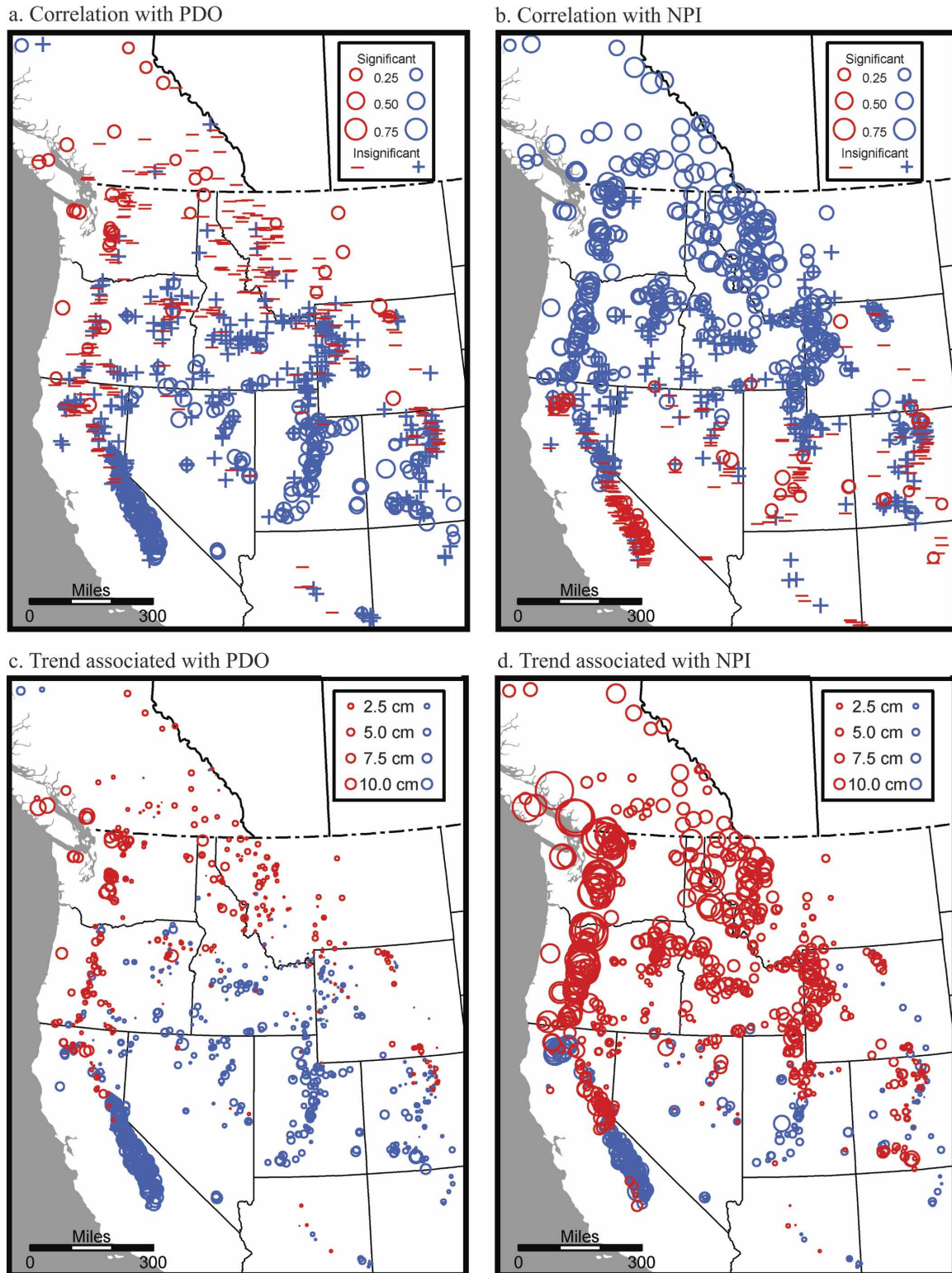


FIG. 8. Relationships between two climate indices, NPI and PDO, and 1 Apr SWE, over the 1960–2002 period of record. (a), (b) Correlations are shown as red for negative and blue for positive; circles indicate statistically significant trends, and + or – indicates insignificant trends. (c), (d) The trend explained by regression with the index,  $\langle \text{SWE} \rangle_x$  [see Eq. (3)], in units of cm as in Fig. 5.

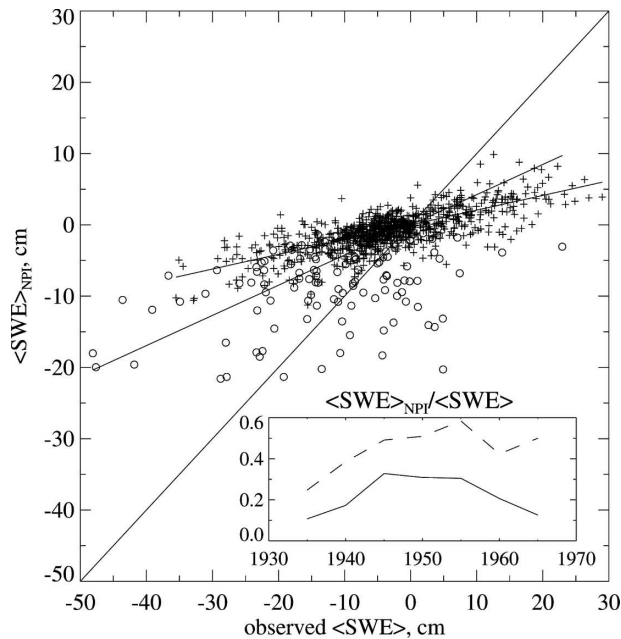


FIG. 9. Scatterplot between absolute trends and trends explained by NPI, that is, between the points on the map in Fig. 5a and the points in Fig. 8d. One line is fitted to PNW points (circles) and one is fitted to non-PNW points (+ symbols). The inset shows how the slopes of the two lines depend on the starting year of the analysis, with the dashed line representing the PNW points.

sented by circles) and one for all the rest of the snow courses. The slope of the line represents the mean fraction of trend attributable to NPI, in this case 0.42 for points in the Pacific Northwest (PNW) and 0.21 for non-PNW points. A few of the snow courses in the PNW with trends between 10 and  $-30$  cm lie near the  $y = x$  line, indicating that those trends can be almost completely explained by the NPI, but the largest negative trends are more typical, with about 20%–40% of the trends explained by NPI. The mean trend for PNW snow courses over 1960–2002 is  $-15$  cm or  $-34\%$ , and for the rest of the West it is  $-9.9$  cm or  $-22\%$ . The inset shows how the slopes of the two fitted lines depend on the starting year, from 1935 when very little of the overall trend could be explained by NPI to 1945–55 when about half of the trend in the PNW and a third of the trend in the rest of the West are explained by NPI. Results are roughly similar for PDO (not shown), except that the slopes of the lines are typically less for PNW than for non-PNW snow courses owing to the smaller correlation with PDO in the PNW.

Plotting the correlations in Fig. 8 as a latitude–altitude transect (Fig. 10) reveals a striking fact about the relationship between these climate indices and SWE: the correlations depend strongly on elevation in California, as well as on latitude from north to south. In

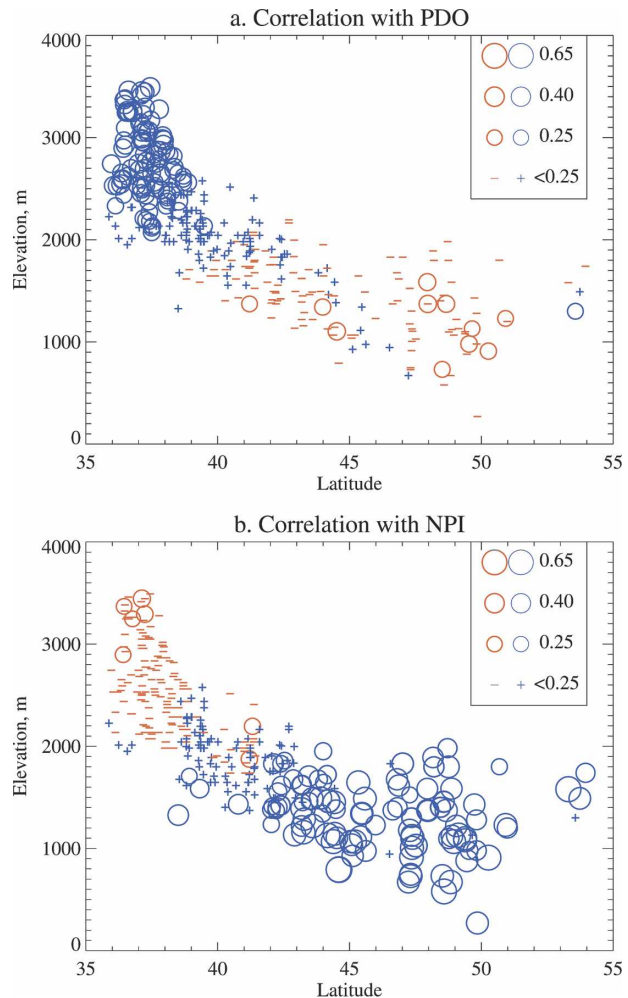


FIG. 10. Transect (as in Fig. 6) of the correlations shown in Figs. 8a,b.

northern California and southern Oregon, higher snow courses are positively (but not significantly) correlated with PDO, while lower snow courses are negatively correlated with PDO. In central and southern California, the strength of the correlation generally increases with altitude. For NPI, the situation is somewhat reversed: in northern California and southern Oregon, most of the lower-elevation snow courses are significantly positively correlated with NPI, and at higher elevations some significant negative correlations emerge. In southern California (south of  $38^\circ\text{N}$ ), a few of the lowest-elevation snow courses are positively (though weakly) correlated with NPI and most of the highest-elevation snow courses are significantly negatively correlated with NPI. These differences can be understood as an interaction between the separate influences of the climate pattern (PDO or NPI) on temperature and on precipitation: at low elevations, temperature matters

most, and temperature is negatively correlated with NPI throughout the transect (see [www.cdc.noaa.gov/USclimate/Correlation](http://www.cdc.noaa.gov/USclimate/Correlation)). At higher elevations, precipitation matters more, and precipitation is (weakly) negatively correlated with NPI in California and positively in the PNW. Thus, the elevationally determined competition between the effects of temperature and the effects of precipitation are convolved with the spatially varying response to NPI (or PDO) to produce this complex pattern of correlations with NPI and PDO.

## 6. Conclusions

The modest success of this simple regression approach suggests that for most snow course locations in the West, the long-term variations in spring SWE are reasonably well explained by summaries of seasonal climate at nearby locations. This implies that day-to-day details of snow accumulation, ablation, and melt are generally of secondary importance, except where correlations between observed SWE and climate-derived SWE are low.

On longer time scales, another implication of the general agreement between observed and climate-derived SWE is that other sources of trends are also generally of secondary importance. Where discrepancies exist, they could be caused by, for example, changes in forest canopy or other aspects of site characteristics that influence SWE, or substantially different climate trends between the relatively low-elevation climate stations and the snow course locations.

During the second half of the twentieth century, and likely even since 1916 (Hamlet et al. 2005), winter and spring warming in the West have reduced spring snowpack at most locations. Increases in precipitation appear to have offset this loss in some places since mid-century, notably in the southern Sierra Nevada mountains, where large increases have occurred. Some of the interannual variability and long-term trends can be explained as a response to variability and change in North Pacific climate, especially as represented by the North Pacific Index (NPI), which responds to the oceanic variations ENSO and PDO. However, NPI can only account for about half of the trends in the PNW since mid-century (and less elsewhere or from earlier starting points), in rough agreement with the modeling results of Hamlet et al. (2005). The remaining portion clearly includes the influence of the monotonic warming (e.g., Fig. 5c) observed throughout the West, which is largely unrelated to Pacific climate variability and may well represent human influence on climate (Karoly and Wu 2005). That is, even after accounting for the role of

known patterns of climate variability, there is a substantial downward trend in overall snowpack in the West that is consistent with the observed warming.

Even a conservative estimate ( $0.3^{\circ}\text{C}/\text{decade}^{-1}$ ) of the likely warming rate for western mountains in winter (Leung et al. 2004) would, by 2100, move the  $0^{\circ}$  isotherm where the  $3^{\circ}\text{C}$  isotherm now lies: most of the westernmost mountains would be in the transient snow zone, in which snow accumulates and melts repeatedly during the snow season. One implication of Fig. 6 is that spring SWE will grow more and more sensitive to temperature. In other words, the more it warms, the more the warming will affect snowpack even at higher elevations. These results underscore those from modeling efforts (e.g., Hamlet and Lettenmaier 1999; Knowles and Cayan 2004), which have illustrated the likely declines in snowpack from a warming climate, but with the added detail that the intraseasonal behavior of snowpack will change from one of steady accumulation to alternating accumulation and loss. Simple regression-based methods for forecasting seasonal volumetric streamflow will have to be revised or replaced by more sophisticated methods that can account for the changing role of temperature both in determining the quantity of spring snowpack (the subject of this paper) and the rate at which it melts (Hamlet et al. 2005).

*Acknowledgments.* I am grateful to Rob Norheim, who expertly constructed the maps. These analyses would not have been possible without the efforts of the dedicated snow surveyors who laboriously collected the data. I thank Alan Hamlet, Dennis Lettenmaier, Mike Wallace, Martyn Clark, Todd Mitchell, and Dan Cayan for helpful discussions and suggestions on an earlier version of this manuscript. This publication is funded by the Joint Institute for the Study of the Atmosphere and Ocean (JISAO) under NOAA Cooperative Agreement No. NA17RJ1232.

## REFERENCES

- Bond, N. A., J. E. Overland, M. Spillane, and P. Staben, 2003: Recent shifts in the state of the North Pacific. *Geophys. Res. Lett.*, **30**, 2183, doi:10.1029/2003GL018597.
- Bowling, L. C., P. Storck, and D. P. Lettenmaier, 2000: Hydrologic effects of logging in western Washington United States. *Water Resour. Res.*, **36**, 3223–3240.
- Cayan, S., A. Kammerdiener, M. D. Dettinger, J. M. Caprio, and D. H. Peterson, 2001: Changes in the onset of spring in the western United States. *Bull. Amer. Meteor. Soc.*, **82**, 399–415.
- Clark, M. P., M. C. Serreze, and G. J. McCabe, 2001: Historical effects of El Niño and La Niña events on the seasonal evolution of the montane snowpack in the Columbia and Colorado River basins. *Water Resour. Res.*, **37**, 741–757.
- Daly, C., R. P. Neilson, and D. L. Phillips, 1994: A statistical-

- topographic model for mapping climatological precipitation over mountain terrain. *J. Appl. Meteor.*, **33**, 140–158.
- Diaz, H. F., and R. S. Bradley, 1997: Temperature variations during the last century at high elevation sites. *Climate Change*, **59**, 33–52.
- Groisman, P. Ya., R. W. Knight, T. R. Karl, D. R. Easterling, B. Sun, and J. H. Lawrimore, 2004: Contemporary changes of the hydrological cycle over the contiguous United States: Trends derived from in situ observations. *J. Hydrometeorol.*, **5**, 64–84.
- Hamlet, A. F., and D. P. Lettenmaier, 1999: Effects of climate change on hydrology and water resources in the Columbia River basin. *J. Amer. Water Resour. Assoc.*, **35**, 1597–1623.
- , and —, 2005: Production of temporally consistent gridded precipitation and temperature fields for the continental United States. *J. Hydrometeorol.*, **6**, 330–336.
- , P. W. Mote, M. P. Clark, and D. P. Lettenmaier, 2005: Effects of temperature and precipitation variability on snowpack trends in the western United States. *J. Climate*, **18**, 4545–4561.
- Karl, T. R., C. N. Williams, Jr., F. T. Quinlan, and T. A. Boden, 1990: United States Historical Climatology Network (HCN) serial temperature and precipitation data. Publication 304, Environmental Sciences Division, Carbon Dioxide Information and Analysis Center, Oak Ridge National Laboratory, Oak Ridge, TN.
- Karoly, D. J., and Q. Wu, 2005: Detection of regional surface temperature trends. *J. Climate*, **18**, 4337–4343.
- Knowles, N., and D. Cayan, 2004: Elevational dependence of projected hydrologic changes in the San Francisco estuary and watershed. *Climate Change*, **62**, 319–336.
- , M. D. Dettinger, and D. R. Cayan, 2006: Trends in snowfall versus rainfall for the western United States. *J. Climate*, **19**, 4545–4554.
- Leung, L. R., Y. Qian, X. Bian, W. M. Washington, J. Han, and J. O. Roads, 2004: Mid-century ensemble regional climate change scenarios for the western United States. *Climate Change*, **62**, 75–113.
- Mantua, N. J., S. R. Hare, Y. Zhang, J. M. Wallace, and R. C. Francis, 1997: A Pacific interdecadal climate oscillation with impacts on salmon production. *Bull. Amer. Meteor. Soc.*, **78**, 1069–1079.
- Mote, P. W., 2003a: Trends in snow water equivalent in the Pacific Northwest and their climatic causes. *Geophys. Res. Lett.*, **30**, 1601, doi:10.1029/2003GL017258.
- , 2003b: Trends in temperature and precipitation in the Pacific Northwest during the twentieth century. *Northwest Sci.*, **77**, 271–282.
- , A. F. Hamlet, M. P. Clark, and D. P. Lettenmaier, 2005: Declining mountain snowpack in western North America. *Bull. Amer. Meteor. Soc.*, **86**, 39–49.
- Pepin, N. C., and D. J. Seidel, 2005: A global comparison of surface and free-air temperatures at high elevations. *J. Geophys. Res.*, **110**, D03104, doi:10.1029/2004JD005047.
- Regonda, S. K., B. Rajagopalan, M. Clark, and J. Pitlick, 2005: Seasonal cycle shifts in hydroclimatology over the western United States. *J. Climate*, **18**, 372–384.
- Scott, D., and D. Kaiser, 2004: Variability and trends in United States snowfall over the last half century. Preprints, *15th Symp. on Global Climate Variations and Change*, Seattle, WA, Amer. Meteor. Soc., CD-ROM, 5.2.
- Stewart, I. T., D. R. Cayan, and M. D. Dettinger, 2005: Changes towards earlier streamflow timing across western North America. *J. Climate*, **18**, 1136–1155.
- Trenberth, K. E., and J. W. Hurrell, 1994: Decadal atmosphere-ocean variations in the Pacific. *Climate Dyn.*, **9**, 303–319.
- Vincent, L. A., and D. W. Gullett, 1999: Canadian historical and homogeneous temperature datasets for climate change analysis. *Int. J. Climatol.*, **19**, 1375–1388.
- von Storch, H., and F. W. Zwiers, 1999: *Statistical Analysis in Climate Research*. Cambridge University Press, 484 pp.